

Improving the Transferability of Adversarial Examples by Inverse Knowledge Distillation

Wenyuan Wu¹, Zheng Liu², Yong Chen³, Chao Su¹, Dezhong Peng¹ and Xu Wang^{1*}

¹College of Computer Science, Sichuan University, China

²Sichuan Newstrong UHD Video Technology Company Ltd., China

³Institute of Optics and Electronics, Chinese Academy of Sciences, China

wuwenyuan97@gmail.com, liuzheng@uptcsc.com, cy1415926@gmail.com, suchao.ml@gmail.com, pengdz@scu.edu.cn, wangxu.scu@gmail.com

Abstract

In recent years, the rapid development of deep neural networks has brought increased attention to the security and robustness of these models. While existing adversarial attack algorithms have demonstrated success in improving adversarial transferability, their performance remains suboptimal due to a lack of consideration for the discrepancies between target and source models. To address this limitation, we propose a novel method, Inverse Knowledge Distillation (IKD), designed to enhance adversarial transferability effectively. IKD introduces a distillation-inspired loss function that seamlessly integrates with gradient-based attack methods, promoting diversity in attack gradients and mitigating overfitting to specific model architectures. By diversifying gradients, IKD enables the generation of adversarial samples with superior generalization capabilities across different models, significantly enhancing their effectiveness in black-box attack scenarios. Extensive experiments on the ImageNet dataset validate the effectiveness of our approach, demonstrating substantial improvements in the transferability and attack success rates of adversarial samples across a wide range of models.

1 Introduction

The rapid advancements and significant achievements in deep learning over the past few years have led to an increased focus on its security aspects. A key security concern is the susceptibility of these systems to minimal, nearly undetectable adversarial noise [Szegedy *et al.*, 2013]. This vulnerability suggests a high risk of deliberate attacks, particularly in technologies such as facial recognition and autonomous driving. Although it is crucial to research methods to bolster deep learning models against adversarial attacks, it is of equal importance to investigate strategies for launching attacks on these models.

Current attack strategies create an adversarial sample by incorporating elaborate adversarial perturbations into the input. These perturbations are usually generated by generat-

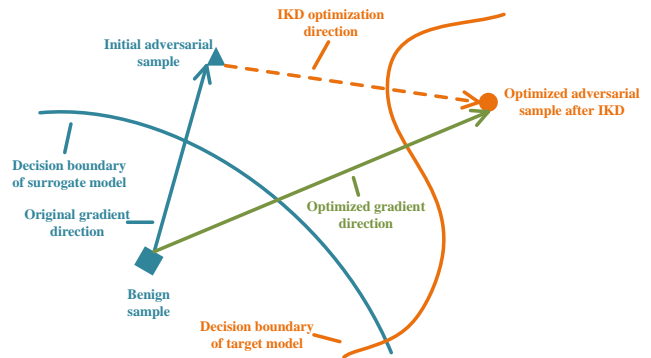


Figure 1: **The distinction between Inverse Knowledge Distillation (IKD) method and existing gradient-based attack approaches.** The blue arrow indicates the gradient direction of traditional gradient-based attack methods, which are heavily reliant on the decision boundary of the surrogate model (i.e., closely correlated with the parameters of the surrogate model). As a result, these methods may fail to effectively attack the target model, as they often cannot generate adversarial samples capable of crossing the decision boundary of the target model, represented by the orange curve. In contrast, by optimizing the attack gradient direction (indicated by the orange dashed line), our IKD method not only ensures that the adversarial sample successfully crosses the surrogate model’s decision boundary, but also increases the likelihood of the adversarial sample overcoming the target model’s decision boundary. Consequently, our IKD method demonstrates a higher success rate in transfer-based attacks.

ing networks [Zhao *et al.*, 2018; Joshi *et al.*, 2019; Qiu *et al.*, 2020; Xiao *et al.*, 2021] or gradient-based optimization techniques [Goodfellow *et al.*, 2014; Madry *et al.*, 2017; Dong *et al.*, 2018; Xie *et al.*, 2019; Dong *et al.*, 2019; Lin *et al.*, 2019]. The latter, the gradient-based approach, is the mainstream. The central idea behind these methods is to generate adversarial perturbations through gradients, which are calculated by maximizing the loss function associated with the target task.

Existing attack methods demonstrate high efficiency in white-box scenarios but face significant challenges in black-box models, where internal model information is inaccessible. This limitation significantly increases the difficulty of attacks. To address this issue, research efforts are primar-

*Corresponding author.

ily categorized into two approaches: query-based attacks and transfer-based attacks. Query-based attacks generate adversarial samples through extensive queries but incur high computational costs and time overhead. In contrast, transfer-based attacks leverage the transferability of adversarial samples, generating them on surrogate models for application to black-box models, offering greater efficiency and practicality. Consequently, this paper focuses on transfer-based attacks, aiming to enhance the transferability of adversarial samples and improve their effectiveness in black-box attack scenarios.

At present, transfer-based attack methods have covered a variety of technologies, including input transformation-based attacks [Dong *et al.*, 2019; Liang and Xiao, 2023; Wang *et al.*, 2021a; Xie *et al.*, 2019], advanced gradient attacks [Dong *et al.*, 2018; Li *et al.*, 2023; Lin *et al.*, 2019; Wang and He, 2021], ensemble attacks [Qian *et al.*, 2023; Tramèr *et al.*, 2017; Xiong *et al.*, 2022], feature-based attacks [Ganeshan *et al.*, 2019; Wang *et al.*, 2023; Zhang *et al.*, 2022], and so on. Although these methods can improve the transferability of attacks to some extent, they usually come with high computational costs. Moreover, existing methods often fail to adequately account for the differences between surrogate models and target models. As a result, the generated adversarial perturbations tend to perform better on surrogate models but may not retain the same effectiveness when applied to target models. Specifically, these methods suffer from a lack of diversity in attack gradients, relying heavily on a single fixed direction to generate adversarial samples while neglecting other potential directions. This fixed direction is typically determined by the computations of the surrogate model, causing the generated adversarial samples to overfit the surrogate model and limiting their effectiveness in attacking the target model.

To address this challenge, we propose Inverse Knowledge Distillation (IKD), a novel and effective method aimed at mitigating overfitting by enhancing gradient diversity. IKD integrates a distillation-inspired mechanism into the loss computation of gradient-based attack methods, optimizing not only the alignment with the specified label but also the divergence in output feature distributions between adversarial and benign samples on the surrogate model. This approach introduces richer gradient information, breaking the constraints of fixed gradient directions and significantly enhancing gradient diversity. As illustrated in Figure 1, by maximizing the difference in feature distributions, IKD reduces dependence on the specific decision boundaries of surrogate models, compelling the optimization process to prioritize more generalized perturbations. This effectively prevents adversarial samples from overfitting to surrogate models and substantially improves their transferability.

The main contributions of our work can be summarized as follows:

- We propose a simple and effective adversarial attack method: Inverse Knowledge Distillation (IKD) attack. IKD can effectively reduce the overfitting problem and enhance the adversarial sample’s transferability. Our Inverse Knowledge distillation (IKD) method is compatible and easy to integrate with gradient-based attack methods to improve attack effectiveness.

- We reveal that different distillation methods have significant differences on the transferability of adversarial perturbations. Compared with mean square error (MSE) and cross-entropy (CE) loss, the KL divergence based distillation method shows the best effect in improving the transferability of the adversarial sample.
- We conducted a large number of experiments on the ImageNet dataset to verify the validity of the proposed IKD method. The experimental results show that the proposed method significantly improves the success rate of almost all attack methods, which proves the potential and advantage of IKD in practice.

2 Related Works

2.1 Adversarial Attack

The primary attack techniques comprise of the generative-based [Zhao *et al.*, 2018; Song *et al.*, 2018; Joshi *et al.*, 2019; Qiu *et al.*, 2020; Xiao *et al.*, 2021], and gradient-based strategies [Goodfellow *et al.*, 2014; Madry *et al.*, 2017; Dong *et al.*, 2018; Xie *et al.*, 2019; Dong *et al.*, 2019; Lin *et al.*, 2019]. FGSM (Fast Gradient Sign Method) [Goodfellow *et al.*, 2014] is a simple and fast method for generating adversarial examples.

Since then, various methods have been proposed to enhance the attacking capability of adversarial samples. In DIM [Xie *et al.*, 2019], randomization operations of random resizing and padding of the original image were introduced. TIM [Dong *et al.*, 2019] proposes a translation-invariant attack method by convolving the gradient with a Gaussian kernel, further augmenting the attacking capability of the samples. Inspired by Nesterov’s accelerated gradient [Nesterov, 1983], SIM [Lin *et al.*, 2019] modified the accumulation of gradients to effectively predict and enhance the adversariality of the samples. VT [Wang and He, 2021] considered the gradient variance of the previous iteration to adjust the current gradient, thereby stabilizing the update direction and avoiding poor local optima. EMI [Wang *et al.*, 2021b] accumulated the gradients of data points sampled in the direction of the previous iteration’s gradient to find a more stable gradient direction. MagicGAN [Chen *et al.*, 2022] devises a multi-agent discriminator capable of adapting to the decision boundaries of diverse target models. This provides a more varied gradient information spectrum, facilitating the creation of adversarial perturbations. MTAA [Chen *et al.*, 2023] employs a representation that preserves relationships to study patterns that are adversarial. APAA [Yuan *et al.*, 2024] directly utilizes the precise gradient direction with a scale factor to generate adversarial perturbations, thereby enhancing the attack success rate of adversarial samples, even with lesser perturbations.

However, none of these methods take into account the effect of the lack of diversity of attack gradients on the adversarial sample’s transferability. Therefore, the adversarial samples generated by these methods are heavily dependent on the specific decision boundaries of the surrogate model, thus reducing the attack effect on the target model.

2.2 Adversarial Defense

The goal of adversarial defense is to enhance the resilience of the target model when adversarial samples serve as inputs. Defense approaches can primarily be classified into three types: adversarial detection, adversarial purification, and adversarial training. Adversarial detection techniques [Wang *et al.*, 2019; Meng and Chen, 2017; Liang *et al.*, 2018; Zheng and Hong, 2018], in most instances, obviate the need for model retraining, thereby substantially reducing the complexity of the undertaking. The detection of adversarial instances hinges on the study of the characteristics of adversarial perturbations and their statistical deviations from normal instances. This approach enables the differentiation of adversarial instances during the operation of DNN models, thereby safeguarding them from potential adversarial attacks. Adversarial purification techniques [Liao *et al.*, 2018; Liu *et al.*, 2019; Jia *et al.*, 2019], typically aim to eliminate noise from adversarial samples before they are input into the classifier. Adversarial training techniques [Madry *et al.*, 2017; Tramèr *et al.*, 2017; Pang *et al.*, 2020], on the other hand, utilize adversarial samples as additional training data to boost the model’s robustness.

3 Method

3.1 Problem Definition

The task of adversarial attack involves making subtle modifications to the original image by introducing imperceptible noise, to cause the target model to misclassify the resulting adversarial samples. For instance, a gradient-based approach generates adversarial samples by maximizing the cross-entropy loss function, and its optimization objective can be expressed as:

$$\arg \max_{x^{adv}} \mathcal{L}(f_{\theta}(x^{adv}), y), \quad s.t. \|x^{adv} - x\|_p \leq \epsilon, \quad (1)$$

where x^{adv} denote the adversarial sample, $x^{adv} = x + \delta$, with x representing the benign sample and δ the adversarial perturbation. y represents the ground truth label. f_{θ} is a well-trained classification model parameterized by θ , and $\mathcal{L}(\cdot, \cdot)$ denotes the cross-entropy loss in the classification task. $\|\cdot\|_p$ represents the l_p -norm. In this study, we continue the previous work [Dong *et al.*, 2019; Li *et al.*, 2023; Xie *et al.*, 2019] and use the l_{∞} norm to measure the size of the adversarial perturbation. In this framework, the maximum allowable correction of the perturbation δ is controlled by ϵ , and the perturbation satisfies a specific constraint, that is, it is in the l_{∞} sphere with radius ϵ centered on x . Specifically, the disturbance δ must satisfy $\|\delta\|_p \leq \epsilon$, which ensures that the adversarial perturbation does not deviate too far from the original sample x , thus ensuring that the generated adversarial sample is reasonable in the input space, while maintaining the effectiveness of the attack.

However, the problem in Equation (1) can only be solved if the classification model is directly accessible, i.e., in a white-box setting. In a black-box scenario, where the target model f_{θ} is not directly accessible, this method cannot be directly applied for attacks. In such cases, directly solving the problem becomes infeasible. To address this limitation, a potential solution is to generate adversarial samples on a surrogate

model f_{φ} and exploit their transferability to attack the inaccessible target model f_{θ} . Given the inherent differences between the surrogate and target models, improving the transferability of adversarial samples generated by the surrogate model f_{φ} is crucial. This is because the transferability of adversarial samples determines their effectiveness across different models. In black-box attacks, for instance, highly transferable adversarial samples can successfully bypass the defenses of the target model. Therefore, the primary focus of this paper is to enhance the transferability of adversarial samples generated by surrogate models.

3.2 Inverse Knowledge Distillation Attack

Knowledge distillation (KD) is a model compression technique that transfers the knowledge of a large, complex model (referred to as the “teacher model”) to a smaller, simpler model (referred to as the “student model”), thereby reducing the computational complexity of the student model while maintaining performance that is close to that of the teacher model [Hinton, 2015]. This method guides the training of the student model by learning from either the output probability distribution or the intermediate representations of the teacher model.

Inspired by knowledge distillation techniques, we propose the Inverse Knowledge Distillation (IKD) method. Unlike knowledge distillation, our IKD attack method does not involve the concepts of teacher and student models, nor does it require the student model to learn from the teacher model. Instead, our approach aims to maximize the disparity between the predictive output $f_{\varphi}(x)$ of the surrogate model f_{φ} on benign input data x and the predictive output $f_{\varphi}(x^{adv})$ of the surrogate model on adversarial input data x^{adv} , without compromising the performance of the white-box adversarial attack. In this case, the optimization objective in Equation (1) becomes the following:

$$\arg \max_{x^{adv}} (\mathcal{L}_{hard}(f_{\varphi}(x^{adv}), y) + \gamma \cdot \mathcal{L}_{soft}(f_{\varphi}(x^{adv}), f_{\varphi}(x))), \quad (2)$$

where γ is the distillation weight. The objective is to minimize the amount of knowledge contained in the adversarial sample x^{adv} that is related to the surrogate model f_{φ} , in order to avoid overfitting of the adversarial sample x^{adv} to the surrogate model f_{φ} and to enhance the transferability of the adversarial sample.

The soft label loss \mathcal{L}_{soft} , defined in Equation (2), can take various common forms, such as Kullback-Leibler (KL) divergence, mean square error (MSE), and cross-entropy (CE). In IKD, we select KL divergence as the soft label loss, formulated as:

$$\begin{aligned} \mathcal{L}_{soft}(f_{\varphi}(x^{adv}), f_{\varphi}(x)) &= KL(f_{\varphi}(x) \| f_{\varphi}(x^{adv})) \\ &= \sum_i f_{\varphi}(x)(i) \log \frac{f_{\varphi}(x)(i)}{f_{\varphi}(x^{adv})(i)}, \end{aligned} \quad (3)$$

The KL divergence measures how much information is lost when $f_{\varphi}(x^{adv})$ is used to approximate $f_{\varphi}(x)$. It provides unique advantages in quantifying the difference between the

probability distributions of benign samples $f_\varphi(x)$ and adversarial samples $f_\varphi(x^{adv})$.

The primary reasons for selecting KL divergence over MSE or CE as the soft label loss are as follows. First, the gradient of KL divergence with respect to $f_\varphi(x^{adv})$ is given by:

$$\frac{\partial KL(f_\varphi(x) \| f_\varphi(x^{adv}))}{\partial f_\varphi(x^{adv})(i)} = -\frac{f_\varphi(x)(i)}{f_\varphi(x^{adv})(i)}, \quad (4)$$

which exhibits two key characteristics: asymmetric sensitivity and probabilistic emphasis. Asymmetric sensitivity refers to the fact that KL divergence penalizes larger deviations of $f_\varphi(x^{adv})$ from $f_\varphi(x)$ more heavily. This asymmetry is crucial for capturing directional differences in the probability distributions, ensuring that adversarial samples move away from the benign sample distribution and, consequently, the decision boundary of the surrogate model. Probabilistic emphasis, on the other hand, means that the gradient is weighted by $f_\varphi(x)$, prioritizing high-probability regions of the benign distribution. This alignment enhances the goal of modifying the adversarial sample’s predictions.

Second, the gradient of MSE with respect to $f_\varphi(x^{adv})$ is given by:

$$\frac{\partial MSE(f_\varphi(x) \| f_\varphi(x^{adv}))}{\partial f_\varphi(x^{adv})(i)} = \frac{2}{N}(f_\varphi(x^{adv}) - f_\varphi(x)). \quad (5)$$

Compared to KL divergence, MSE has two main drawbacks: symmetric penalization and gradient uniformity. Symmetric penalization refers to the fact that MSE treats overestimation and underestimation of probabilities symmetrically, which is suboptimal for adversarial attacks. Gradient uniformity means that MSE does not account for the relative importance of the probability $f_\varphi(x^{adv})$. As a result, MSE applies uniform penalties across all categories, diminishing its effectiveness in optimizing the high-probability regions of the target distribution. Consequently, MSE lacks the probabilistic emphasis and asymmetric sensitivity needed for generating effective adversarial attacks.

Finally, the gradient of Cross-Entropy (CE) with respect to $f_\varphi(x^{adv})$ is given by:

$$\frac{\partial CE(f_\varphi(x) \| f_\varphi(x^{adv}))}{\partial f_\varphi(x^{adv})(i)} = -\frac{f_\varphi(x)(i)}{f_\varphi(x^{adv})(i)}. \quad (6)$$

Although both CE and KL divergence share the same gradient structure, they differ in their original forms. In CE, the rightmost logarithmic term is $\log f_\varphi(x^{adv})$, whereas in KL divergence, it is $\log \frac{f_\varphi(x)}{f_\varphi(x^{adv})}$. This difference introduces two key disadvantages for CE. First, CE cannot capture the relationship between $f_\varphi(x)$ and $f_\varphi(x^{adv})$ when $f_\varphi(x)$ is close to zero. In such cases, CE fails to fully account for the deviation of $f_\varphi(x^{adv})$, potentially leading to suboptimal gradient updates. Second, CE only focuses on the direction from $f_\varphi(x^{adv})$ to $f_\varphi(x)$. In contrast, the mutual penalization in KL divergence ensures that both $f_\varphi(x)$ and $f_\varphi(x^{adv})$ are pushed away from each other in a balanced manner, a property that CE lacks.

Additionally, a series of experiments are conducted to validate the effectiveness of selecting KL divergence as the soft label loss, as detailed in Section 4.3.

3.3 Enhanced Gradient Diversity

The introduction of the IKD enhances the diversity of gradients used during the adversarial example generation. Traditional gradient-based attack methods, such as FGSM and I-FGSM, often rely on the gradient of the loss with respect to the input, which can lead to similar perturbations along specific directions of the input space.

To address this issue, we introduce IKD into the loss calculation. This modification ensures that, in addition to the gradient of the classification loss with respect to the input, the optimization process now incorporates the gradient of the divergence between the distributions of benign and adversarial examples. This additional term encourages the attack to move not only along the steepest descent direction of the adversarial loss but also in directions that maximize the difference between the output distributions of the benign and adversarial samples. As a result, the adversarial example is pushed to explore a broader range of directions in the input space, leading to greater gradient diversity.

This increased gradient diversity prevents the optimization from getting stuck in local minima and allows the adversarial perturbations to better generalize across different models, which is essential for improving transferability.

3.4 Attack Algorithm

Similar to previous work [Xie *et al.*, 2019; Long *et al.*, 2022], the proposed method can be seamlessly integrated with any gradient-based attack technique. For instance, using MIFGSM as an example, we combine inverse knowledge distillation (IKD) with MIFGSM to introduce a new attack method, named MIFGSM-IKD. In this process, inverse distillation is incorporated into the gradient update rules of the MIFGSM attack to improve the transferability of adversarial samples. Specifically, by introducing IKD into the loss function, inverse distillation adjusts the gradient update direction, enabling the generated adversarial samples to not only effectively attack the surrogate model but also exhibit enhanced cross-model transferability. We propose a new adversarial sample update formula for the MIFGSM-IKD method, as follows:

$$\begin{aligned} x_0^{adv} &= x, g_0 = 0, \\ \mathcal{L}_{total} &= \mathcal{L}_{hard}(f_\varphi(x^{adv}), y) + \gamma \mathcal{L}_{soft}(f_\varphi(x^{adv}), f_\varphi(x)), \\ g_{t+1} &= \mu \cdot g_t + \frac{\nabla_x(\mathcal{L}_{total})}{\|\nabla_x(\mathcal{L}_{total})\|_1}, \\ x_{t+1}^{adv} &= x_t^{adv} + \alpha \cdot \text{sign}(g_{t+1}), \end{aligned} \quad (7)$$

where g_t and x_t^{adv} represent the gradient and the adversarial sample generated at the t -th iteration, respectively. The parameter α denotes the attack step size and controls the magnitude of the update to the adversarial sample in each iteration. μ is an attenuation factor used to adjust the influence of historical information during gradient updating. $\|\cdot\|_1$ represents the L_1 norm. Thus, the IKD can be applied as an enhancement to the gradient-based attack method to improve its effectiveness in black-box settings.

Table 1: Comparison results of various attack methods in terms of attack success rate (%). The bold item indicates the best one. Item with * superscript is white-box attacks, and the others is black-box attacks. AVG column indicates the average attack success rate on black-box models.

Source Model	Method	Target Model											
		RN50	DN121	RNX50	VGG19BN	IncRes-v2	Inc-v3	Inc-v4	RN101	RN152	Inc-v3 _{adv}	IncRes-V2 _{adv,ens}	AVG
RN50	MIFGSM	99.9*	65.7	75.2	73.2	38.9	52.6	46.0	68.2	62.1	30.6	16.0	52.9
	MIFGSM-IKD	99.9*	68.4	79.4	76.0	39.9	54.4	49.6	73.1	67.6	32.1	16.3	55.7
	DIFGSM	99.9*	82.9	88.8	84.7	61.7	70.3	69.4	86.1	82.1	35.9	18.4	68.0
	DIFGSM-IKD	99.8*	84.9	90.6	84.8	62.9	70.8	69.6	86.5	83.3	38.4	18.9	69.1
	TIFGSM	99.0*	68.4	65.4	71.3	51.1	63.9	60.3	55.6	49.8	52.8	43.0	58.2
	TIFGSM-IKD	99.2*	69.1	67.1	70.8	52.1	64.5	61.4	57.9	49.5	52.8	43.8	58.9
	NIFGSM	99.9*	71.6	80.0	76.5	43.4	55.2	49.2	75.9	70.7	31.6	16.0	57.0
	NIFGSM-IKD	100.0*	76.5	85.0	79.3	44.6	57.8	52.5	81.1	74.7	32.0	15.4	59.9
DN121	MIFGSM	75.7	100.0*	71.6	86.3	52.2	65.4	58.4	61.4	55.4	38.2	20.9	58.6
	MIFGSM-IKD	78.3	100.0*	76.6	88.5	55.7	70.9	64.1	68.1	62.8	38.6	21.0	62.5
	DIFGSM	87.2	100.0*	84.5	92.0	74.3	82.8	80.2	77.8	72.5	48.5	29.0	72.9
	DIFGSM-IKD	89.0	100.0*	88.5	93.9	77.3	82.7	82.9	81.9	78.6	48.3	29.0	75.2
	TIFGSM	58.4	99.7*	52.8	82.0	60.4	72.8	66.2	40.7	34.1	64.5	54.4	58.6
	TIFGSM-IKD	60.5	99.8*	56.1	81.7	62.1	72.4	67.2	41.3	37.8	65.7	57.5	60.2
	NIFGSM	79.0	100.0*	77.9	86.1	55.3	68.2	62.1	67.3	60.4	39.0	20.4	61.6
	NIFGSM-IKD	82.3	100.0*	80.0	89.4	57.9	70.5	64.8	71.9	66.4	39.6	20.6	64.3
VGG19BN	MIFGSM	47.9	58.9	43.4	100.0*	30.1	46.8	42.9	33.3	28.9	26.6	15.2	37.4
	MIFGSM-IKD	55.2	63.8	50.2	100.0*	34.3	52.5	49.0	39.3	36.4	27.1	14.9	42.3
	DIFGSM	63.3	75.0	58.3	100.0*	46.7	64.5	61.2	46.1	43.1	32.7	18.6	51.0
	DIFGSM-IKD	71.1	80.3	67.9	100.0*	55.8	69.4	69.5	57.4	52.7	35.4	18.6	57.8
	TIFGSM	40.2	59.8	34.6	100.0*	40.5	62.6	56.8	25.2	20.9	44.1	33.8	41.9
	TIFGSM-IKD	44.8	66.2	42.2	100.0*	48.2	65.9	61.6	30.1	26.3	48.8	36.5	47.1
	NIFGSM	54.3	62.9	47.7	100.0*	34.4	50.6	45.2	39.7	33.9	25.9	14.2	40.9
	NIFGSM-IKD	57.8	65.8	51.5	100.0*	36.4	53.5	50.0	41.8	37.0	26.3	14.7	43.5
IncRes-v2	MIFGSM	54.8	64.4	55.2	78.6	98.9*	74.1	70.9	46.4	44.2	44.8	28.0	56.1
	MIFGSM-IKD	58.1	68.7	57.5	79.5	98.9*	77.6	75.0	51.4	47.8	46.3	30.4	59.2
	DIFGSM	64.8	75.2	65.4	82.5	98.6*	84.5	83.9	58.9	54.6	54.7	39.0	66.4
	DIFGSM-IKD	69.7	79.4	69.3	85.3	98.3*	85.7	86.5	64.3	58.4	58.1	39.5	69.6
	TIFGSM	40.9	59.1	39.4	68.0	97.7*	74.3	70.1	31.5	27.4	67.6	63.9	54.2
	TIFGSM-IKD	45.0	60.4	40.9	68.6	97.6*	76.1	73.1	35.6	29.3	70.8	68.2	56.8
	NIFGSM	55.8	65.9	56.2	78.1	99.3*	74.1	70.5	48.6	45.5	43.3	26.6	56.5
	NIFGSM-IKD	60.5	70.3	59.7	80.4	99.4*	76.6	73.3	52.4	50.1	46.9	27.0	59.7
RN101	MIFGSM	72.5	66.3	70.4	74.8	36.9	49.3	44.0	97.4*	70.1	29.4	14.5	52.8
	MIFGSM-IKD	75.3	66.9	72.4	75.1	37.3	50.3	44.4	97.7*	71.7	30.3	14.9	53.9
	DIFGSM	77.7	75.4	77.6	80.6	56.6	63.6	61.0	93.2*	76.6	35.1	17.9	62.2
	DIFGSM-IKD	78.5	75.0	80.1	80.3	56.0	64.5	61.7	93.3*	78.4	32.3	17.7	62.5
	TIFGSM	53.6	56.0	54.0	64.6	44.6	55.0	52.9	77.9*	49.7	42.9	36.3	51.0
	TIFGSM-IKD	53.2	54.7	53.2	64.3	44.3	56.5	53.5	79.8*	50.6	43.5	35.6	50.9
	NIFGSM	79.7	72.2	77.0	78.2	37.9	51.5	45.6	99.2*	74.1	30.1	14.3	56.1
	NIFGSM-IKD	80.3	72.8	77.7	79.2	39.9	52.4	47.6	99.0*	75.1	29.5	15.7	57.0

4 Experiments

4.1 Experiments Setting

Dataset

We use a subset¹ of the ImageNet dataset [Russakovsky *et al.*, 2015] for the experiment. This subset consists of 1,000 images, covering nearly all the major categories in ImageNet, and has been widely used in previous related studies. In the experimental setup, we choose a pixel value range of 0-255 and set the maximum perturbation budget to 16, using the L_∞ norm for the disturbance. Specifically, the perturbation size is constrained such that the adversarial perturbation must satisfy $\|\delta\|_\infty \leq 16$, ensuring that the generated adversarial sample does not deviate significantly from the original sample. Additionally, to match the standardized input format, we adjust the image resolution to $3 \times 224 \times 224$, which complies with the standard preprocessing requirements of the ImageNet dataset.

Evaluation Models

We evaluate all attack methods using conventional training models and defense models. A total of 9 standard models

and 2 defense models, provided by the timm package [Wightman, 2019], are assessed. Specifically, the models used include: ResNet50 [He *et al.*, 2016a], DenseNet121 [Huang *et al.*, 2017], ResNeXt50 [Xie *et al.*, 2017], VGG19BN [Simonyan, 2014], InceptionResNet-v2 [Szegedy *et al.*, 2017], Inception-v3 [Szegedy *et al.*, 2016], Inception-v4 [Szegedy *et al.*, 2017], ResNet101 [He *et al.*, 2016b], ResNet152 [He *et al.*, 2016b], Inception-v3_{adv} [Tramèr *et al.*, 2017] and InceptionResNet-v2_{adv,ens} [Tramèr *et al.*, 2017].

Metrics

To evaluate the effectiveness of different attack methods, we use the attack success rate (ASR) for both white-box and black-box models as measurement indicators.

Baselines

To thoroughly evaluate our proposed approach, we selected several existing baseline attack methods for comparison, including MIFGSM [Dong *et al.*, 2018], DIFGSM [Xie *et al.*, 2019], TIFGSM [Dong *et al.*, 2019], NIFGSM [Lin *et al.*, 2019], SINIFGSM [Lin *et al.*, 2019], VMIFGSM [Wang and He, 2021], and VNIFGSM [Wang and He, 2021]. These methods encompass various types of gradient-based attacks, providing a broad frame of reference to effectively demon-

¹<https://drive.google.com/drive/folders/1CfobY6i8BfqfWPHL31FKFDipNjqWwAhS>

Table 2: Evaluation results of the advanced attacks combined with IKD in terms of attack success rate (%). The bold item indicates the best one. Item with \star superscript is white-box attacks, and the others is black-box attacks. AVG column indicates the average attack success rate on black-box models.

Source Model	Method	Target Model											AVG
		RN50	DN121	RNX50	VGG19BN	IncRes-v2	Inc-v3	Inc-v4	RN101	RN152	Inc-v3 _{adv}	IncRes-V2 _{adv,ens}	
RN50	SINIFGSM	99.9 \star	81.7	85.0	84.5	53.2	67.0	59.3	80.1	75.4	37.6	17.1	64.1
	SINIFGSM-IKD	100.0\star	88.5	91.3	88.7	58.0	69.9	64.5	87.9	84.1	38.2	17.7	68.9
	VMIFGSM	99.9 \star	84.7	88.6	86.5	64.8	73.6	73.5	85.5	84.9	43.8	24.2	71.0
	VMIFGSM-IKD	99.9 \star	86.1	89.3	86.1	65.6	72.6	72.6	87.1	85.3	44.7	23.4	71.3
	VNIFGSM	99.9\star	86.2	89.2	87.0	68.7	74.1	73.1	87.2	86.0	45.0	23.0	72.0
DN121	SINIFGSM	81.2	100.0 \star	77.0	92.7	63.0	77.7	70.6	69.8	64.6	47.8	27.8	67.2
	SINIFGSM-IKD	87.3	100.0 \star	85.5	94.2	68.2	79.5	75.4	77.0	73.0	49.2	29.3	71.9
	VMIFGSM	87.3	100.0 \star	84.6	92.6	73.3	82.6	79.4	79.5	76.7	49.7	34.0	74.0
	VMIFGSM-IKD	88.7	100.0 \star	87.3	93.8	74.4	82.4	81.7	82.5	78.9	50.1	34.9	75.5
	VNIFGSM	87.7	100.0 \star	86.2	93.5	74.1	83.7	80.6	81.1	78.7	49.6	34.1	74.9
VGG19BN	SINIFGSM	55.3	66.0	49.5	100.0 \star	38.3	57.4	50.6	39.3	33.9	31.2	16.6	43.8
	SINIFGSM-IKD	61.6	71.9	55.5	100.0 \star	39.3	59.8	54.2	44.7	40.9	28.9	15.5	47.2
	VMIFGSM	69.9	80.7	63.5	100.0 \star	53.4	70.9	67.5	52.3	48.3	37.1	20.5	56.4
	VMIFGSM-IKD	73.9	83.2	67.6	100.0 \star	54.2	71.5	69.6	57.4	53.2	37.2	19.7	58.8
	VNIFGSM	71.5	81.2	63.7	100.0 \star	53.6	71.9	68.4	54.0	49.8	37.0	20.7	57.2
IncRes-v2	SINIFGSM	64.9	76.1	62.6	85.9	99.8 \star	88.0	79.6	55.7	52.4	61.2	40.9	66.7
	SINIFGSM-IKD	72.9	82.8	69.8	90.5	99.9\star	90.8	86.4	64.2	62.4	66.0	44.6	73.0
	VMIFGSM	63.1	72.3	63.1	81.6	98.8 \star	82.8	82.4	57.0	56.2	57.2	42.7	65.8
	VMIFGSM-IKD	69.7	77.0	69.9	85.2	98.9\star	86.6	86.6	63.5	63.2	61.0	46.9	71.0
	VNIFGSM	66.3	75.1	65.1	82.6	99.5\star	83.9	84.5	59.1	56.2	57.8	41.9	67.3
RN101	SINIFGSM	90.7	87.5	90.6	88.3	64.4	71.8	71.6	99.9\star	89.9	39.0	18.8	71.3
	SINIFGSM-IKD	91.4	88.0	90.9	88.4	65.1	73.2	71.9	99.7 \star	90.4	38.1	19.7	71.7
	VMIFGSM	78.9	74.8	77.9	80.0	58.4	65.3	64.1	95.9 \star	78.3	38.2	23.5	63.9
	VMIFGSM-IKD	79.2	74.9	78.4	79.5	59.0	66.3	64.1	96.1\star	78.4	37.9	23.7	64.1
	VNIFGSM	79.9	76.0	80.5	81.8	59.9	67.2	64.3	96.8 \star	80.4	37.6	24.0	65.2
VGG19BN	VNIFGSM-IKD	81.5	78.1	81.4	81.3	60.7	67.5	65.2	96.8 \star	80.7	39.8	23.3	66.0

strate the performance of our approach against multiple attack strategies.

Implementation Details

To ensure the comparability and consistency of the experiments, we set the maximum permissible perturbation $\epsilon = 16$, the number of iterations $T = 10$, the attack step size $\alpha = \frac{2}{255}$, and the momentum term attenuation factor $\mu = 1.0$, following previous research [Dong *et al.*, 2019; Wang and He, 2021; Xie *et al.*, 2019]. These parameter settings are consistent with those commonly used in the literature, enabling a fair comparison of different attack methods. To facilitate the implementation and comparison of attack strategies, we employ the attack toolkit Torchattacks [Kim, 2020] and retain its default parameters, with the exception of the custom settings for ϵ and T . This ensures that all methods are compared within the same attack framework, minimizing the influence of other factors on the experimental outcomes. All experiments are implemented in the PyTorch framework and executed on one NVIDIA GeForce RTX 3090 GPU.

4.2 Experiments Results

In this section, we integrate the proposed Inverse Knowledge Distillation (IKD) method with existing attack strategies to investigate potential improvements in attack performance. The resulting combined methods are denoted by the suffix “-IKD”, such as MIFGSM-IKD. The comparison methods include classical attacks (e.g., MIFGSM and NIFGSM), attacks based on input transformations (e.g., DIFGSM and TIFGSM), and advanced gradient-based attacks (e.g., SINIFGSM, VMIFGSM, and VNIFGSM).

Combination with classical attacks and attacks based on input transformations

As shown in Table 1, our method outperforms the comparison methods on the vast majority of black-box models. Specifically, we observe a significant improvement in average transferability across almost all eleven models tested. Notably, our method achieves a 6.8% increase in average transferability compared to DIFGSM on the VGG19BN model, with our DIFGSM-IKD method attaining an average transferability of 57.8%, while DIFGSM alone achieves 51.0%. Furthermore, our approach also outperforms most comparison methods under defense models in terms of average attack success rate, demonstrating the effectiveness of our method in attacking defensive mechanisms. Additionally, we find that DenseNet121 is the most vulnerable model, exhibiting the highest average transferability, which challenges the conventional belief that deeper models are inherently more robust than shallower ones. This observation suggests that model robustness is more closely linked to architectural design than to depth alone. Finally, we acknowledge that in some cases, our method may show slightly lower performance than comparison methods in either white-box or black-box settings. This may be due to the introduction of the IKD, which could slightly interfere with the generation of adversarial perturbations. Additional experimental results can be found in the supplementary material.

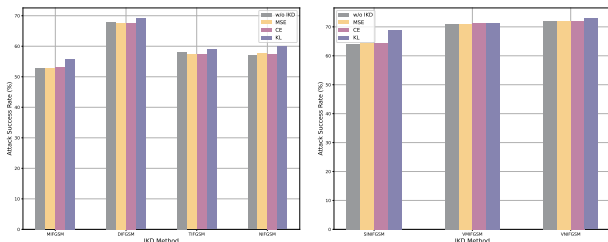
Combination with Advanced gradient Attack

In Table 2, we examine the potential enhancement of attack performance by integrating our approach with advanced gradient-based attacks. On one hand, our method in-

creases the average transferability of the original attack in the vast majority of cases. Specifically, we observe a maximum improvement of 6.3% when using SINIFGSM on the InceptionResNet-v2 model. On the other hand, the performance improvement varies across different attacks and models. For instance, among the eleven models, ResNet50 exhibits the largest increase in attack performance, with a 4.5% improvement. SINIFGSM-IKD achieves a 4.8% increase, while VMIFGSM-IKD shows a modest 0.3% improvement. In contrast, the smallest difference in performance improvement is observed with ResNet101, where the improvement is only 0.6%. Additionally, VNIFGSM-IKD demonstrates the largest performance improvement of 3.4% against DenseNet121 (the best-performing model), and a smaller improvement of 1.6% against VGG19BN (the least improved model) among the four attacks. In comparison, VMIFGSM-IKD shows the smallest variation in performance improvement, with a 0.8% difference between VGG19BN (2.3%) and DenseNet121 (1.5%). This discrepancy may be attributed to the fact that VMIFGSM has less room for improvement relative to other attacks. Additional experimental results can be found in the supplementary material.

4.3 Ablation Study

To thoroughly investigate the potential factors that may influence the performance of our method, we conduct two ablation experiments in this section: (1) the effect of IKD’s soft label loss selection in inverse knowledge distillation, and (2) the impact of the weight of the IKD.

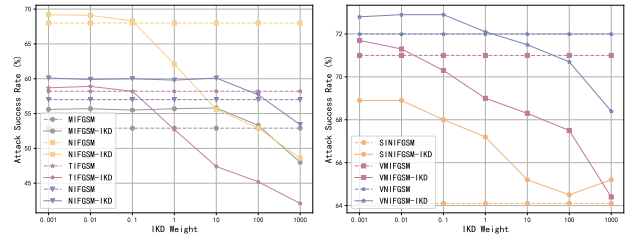


(a) Classical attacks and input transformation-based attacks. (b) Advanced gradient attacks.

Figure 2: Effect of different IKD methods on the transfer-based average attack success rate.

Influence of soft label loss selection on IKD

To investigate the effect of different types of IKD’s soft label loss on adversarial transferability, we employ Mean Squared Error (MSE), Cross-Entropy (CE), and Kullback-Leibler (KL) Divergence for inverse knowledge distillation. Specifically, we conduct experiments on ResNet50 (RN50) using MSE, CE, and KL divergence as the soft label loss in IKD. The average evaluation results are presented in Figure 2. From the results, it is evident that KL divergence demonstrates superior adversarial transferability on RN50 compared to the other two methods. For RN50, the mean transferability with MSE, CE, and KL divergence as the IKD’s soft label



(a) Classical attacks and input transformation-based attacks. (b) Advanced gradient attacks.

Figure 3: Effect of IKD weight on the transfer-based average attack success rate.

loss were 63.2%, 63.4%, and 65.2%, respectively. The transferability across different soft label loss varies significantly. Based on these findings, we opt to use KL divergence as the soft label loss for IKD. For more detailed experimental results, please refer to the supplementary material.

Influence of weight of IKD

The inverse knowledge distillation method exhibits varying influences on the gradient direction based on the weight parameter, which in turn affects the adversarial transferability. To investigate this relationship, we perform a grid search over the weight parameter γ of inverse knowledge distillation in the range $\{0.001, 0.01, 0.1, 1, 10, 100, 1000\}$, using ResNet50 (RN50) as the surrogate model. The average evaluation results are presented in Figure 3. As observed, with the increase in the IKD weight, the average transferability of RN50 initially remains stable within a certain range, and then gradually declines. This suggests that the inverse knowledge distillation method proposed in this paper is not confined to a specific weight value. Based on these findings, we select $\gamma = 0.01$ as the weight for the inverse knowledge distillation attack. For more detailed experimental results, please refer to the supplementary material.

5 Conclusion

In this paper, we propose an inverse knowledge distillation (IKD) method aimed at significantly improving the transferability of adversarial samples. Specifically, we enhance the diversity of attack gradients by incorporating the IKD’s soft label loss into the model’s loss function. IKD not only encourages the model to focus on the classification error of the target label during adversarial sample generation but also optimizes the gradient update direction through the inverse knowledge distillation process. As a result, our approach effectively mitigates overfitting and enhances the transferability of adversarial samples. The proposed IKD method integrates seamlessly with existing gradient-based attack techniques, thereby boosting attack performance. Experimental results demonstrate the efficacy of the proposed method, with extensive evaluations on the ImageNet dataset confirming significant improvements in attack success rates across several baseline attack strategies.

References

- [Chen *et al.*, 2022] Yong Chen, Xu Wang, Peng Hu, and Dezhong Peng. Magicgan: multiagent attacks generate interferential category via gan. *Knowledge-Based Systems*, 258:110023, 2022.
- [Chen *et al.*, 2023] Yong Chen, Xu Wang, Peng Hu, Zhong Yuan, Dezhong Peng, and Qilin Li. Learning relationship-preserving representation for multi-task adversarial attacks. *Neurocomputing*, 554:126580, 2023.
- [Dong *et al.*, 2018] Yinpeng Dong, Fangzhou Liao, Tianyu Pang, Hang Su, Jun Zhu, Xiaolin Hu, and Jianguo Li. Boosting adversarial attacks with momentum. In *Proceedings of the IEEE conference on computer vision and pattern recognition*, pages 9185–9193, 2018.
- [Dong *et al.*, 2019] Yinpeng Dong, Tianyu Pang, Hang Su, and Jun Zhu. Evading defenses to transferable adversarial examples by translation-invariant attacks. In *Proceedings of the IEEE/CVF conference on computer vision and pattern recognition*, pages 4312–4321, 2019.
- [Ganeshan *et al.*, 2019] Aditya Ganeshan, Vivek BS, and R Venkatesh Babu. Fda: Feature disruptive attack. In *Proceedings of the IEEE/CVF International Conference on Computer Vision*, pages 8069–8079, 2019.
- [Goodfellow *et al.*, 2014] Ian J Goodfellow, Jonathon Shlens, and Christian Szegedy. Explaining and harnessing adversarial examples. *arXiv preprint arXiv:1412.6572*, 2014.
- [He *et al.*, 2016a] Kaiming He, Xiangyu Zhang, Shaoqing Ren, and Jian Sun. Deep residual learning for image recognition. In *Proceedings of the IEEE conference on computer vision and pattern recognition*, pages 770–778, 2016.
- [He *et al.*, 2016b] Kaiming He, Xiangyu Zhang, Shaoqing Ren, and Jian Sun. Identity mappings in deep residual networks. In *Computer Vision—ECCV 2016: 14th European Conference, Amsterdam, The Netherlands, October 11–14, 2016, Proceedings, Part IV 14*, pages 630–645. Springer, 2016.
- [Hinton, 2015] Geoffrey Hinton. Distilling the knowledge in a neural network. *arXiv preprint arXiv:1503.02531*, 2015.
- [Huang *et al.*, 2017] Gao Huang, Zhuang Liu, Laurens Van Der Maaten, and Kilian Q Weinberger. Densely connected convolutional networks. In *Proceedings of the IEEE conference on computer vision and pattern recognition*, pages 4700–4708, 2017.
- [Jia *et al.*, 2019] Xiaojun Jia, Xingxing Wei, Xiaochun Cao, and Hassan Foroosh. Comdefend: An efficient image compression model to defend adversarial examples. In *Proceedings of the IEEE/CVF conference on computer vision and pattern recognition*, pages 6084–6092, 2019.
- [Joshi *et al.*, 2019] Ameya Joshi, Amitangshu Mukherjee, Soumik Sarkar, and Chinmay Hegde. Semantic adversarial attacks: Parametric transformations that fool deep classifiers. In *Proceedings of the IEEE/CVF international conference on computer vision*, pages 4773–4783, 2019.
- [Kim, 2020] Hoki Kim. Torchattacks: A pytorch repository for adversarial attacks. *arXiv preprint arXiv:2010.01950*, 2020.
- [Li *et al.*, 2023] Chao Li, Wen Yao, Handing Wang, and Tingsong Jiang. Adaptive momentum variance for attention-guided sparse adversarial attacks. *Pattern Recognition*, 133:108979, 2023.
- [Liang and Xiao, 2023] Kaisheng Liang and Bin Xiao. Styleless: boosting the transferability of adversarial examples. In *Proceedings of the IEEE/CVF Conference on Computer Vision and Pattern Recognition*, pages 8163–8172, 2023.
- [Liang *et al.*, 2018] Bin Liang, Hongcheng Li, Miaoqiang Su, Xirong Li, Wenchang Shi, and Xiaofeng Wang. Detecting adversarial image examples in deep neural networks with adaptive noise reduction. *IEEE Transactions on Dependable and Secure Computing*, 18(1):72–85, 2018.
- [Liao *et al.*, 2018] Fangzhou Liao, Ming Liang, Yinpeng Dong, Tianyu Pang, Xiaolin Hu, and Jun Zhu. Defense against adversarial attacks using high-level representation guided denoiser. In *Proceedings of the IEEE conference on computer vision and pattern recognition*, pages 1778–1787, 2018.
- [Lin *et al.*, 2019] Jiadong Lin, Chuanbiao Song, Kun He, Liwei Wang, and John E Hopcroft. Nesterov accelerated gradient and scale invariance for adversarial attacks. *arXiv preprint arXiv:1908.06281*, 2019.
- [Liu *et al.*, 2019] Zihao Liu, Qi Liu, Tao Liu, Nuo Xu, Xue Lin, Yanzhi Wang, and Wujie Wen. Feature distillation: Dnn-oriented jpeg compression against adversarial examples. In *2019 IEEE/CVF Conference on Computer Vision and Pattern Recognition (CVPR)*, pages 860–868. IEEE, 2019.
- [Long *et al.*, 2022] Yuyang Long, Qilong Zhang, Boheng Zeng, Lianli Gao, Xianglong Liu, Jian Zhang, and Jingkuan Song. Frequency domain model augmentation for adversarial attack. In *European conference on computer vision*, pages 549–566. Springer, 2022.
- [Madry *et al.*, 2017] Aleksander Madry, Aleksandar Makelov, Ludwig Schmidt, Dimitris Tsipras, and Adrian Vladu. Towards deep learning models resistant to adversarial attacks. *arXiv preprint arXiv:1706.06083*, 2017.
- [Meng and Chen, 2017] Dongyu Meng and Hao Chen. Magnet: a two-pronged defense against adversarial examples. In *Proceedings of the 2017 ACM SIGSAC conference on computer and communications security*, pages 135–147, 2017.
- [Nesterov, 1983] Yurii Nesterov. A method for unconstrained convex minimization problem with the rate of convergence $O(1/k^2)$. In *Dokl. Akad. Nauk. SSSR*, volume 269, page 543, 1983.
- [Pang *et al.*, 2020] Tianyu Pang, Xiao Yang, Yinpeng Dong, Kun Xu, Jun Zhu, and Hang Su. Boosting adversarial training with hypersphere embedding. *Advances in Neural Information Processing Systems*, 33:7779–7792, 2020.

- [Qian *et al.*, 2023] Yaguan Qian, Shuke He, Chenyu Zhao, Jiaqiang Sha, Wei Wang, and Bin Wang. Lea2: A lightweight ensemble adversarial attack via non-overlapping vulnerable frequency regions. In *Proceedings of the IEEE/CVF International Conference on Computer Vision*, pages 4510–4521, 2023.
- [Qiu *et al.*, 2020] Haonan Qiu, Chaowei Xiao, Lei Yang, Xinchun Yan, Honglak Lee, and Bo Li. Semanticadv: Generating adversarial examples via attribute-conditioned image editing. In *Computer Vision—ECCV 2020: 16th European Conference, Glasgow, UK, August 23–28, 2020, Proceedings, Part XIV 16*, pages 19–37. Springer, 2020.
- [Russakovsky *et al.*, 2015] Olga Russakovsky, Jia Deng, Hao Su, Jonathan Krause, Sanjeev Satheesh, Sean Ma, Zhiheng Huang, Andrej Karpathy, Aditya Khosla, Michael Bernstein, et al. Imagenet large scale visual recognition challenge. *International journal of computer vision*, 115:211–252, 2015.
- [Simonyan, 2014] Karen Simonyan. Very deep convolutional networks for large-scale image recognition. *arXiv preprint arXiv:1409.1556*, 2014.
- [Song *et al.*, 2018] Yang Song, Rui Shu, Nate Kushman, and Stefano Ermon. Constructing unrestricted adversarial examples with generative models. *Advances in neural information processing systems*, 31, 2018.
- [Szegedy *et al.*, 2013] Christian Szegedy, Wojciech Zaremba, Ilya Sutskever, Joan Bruna, Dumitru Erhan, Ian Goodfellow, and Rob Fergus. Intriguing properties of neural networks. *arXiv preprint arXiv:1312.6199*, 2013.
- [Szegedy *et al.*, 2016] Christian Szegedy, Vincent Vanhoucke, Sergey Ioffe, Jon Shlens, and Zbigniew Wojna. Rethinking the inception architecture for computer vision. In *Proceedings of the IEEE conference on computer vision and pattern recognition*, pages 2818–2826, 2016.
- [Szegedy *et al.*, 2017] Christian Szegedy, Sergey Ioffe, Vincent Vanhoucke, and Alexander Alemi. Inception-v4, inception-resnet and the impact of residual connections on learning. In *Proceedings of the AAAI conference on artificial intelligence*, volume 31, 2017.
- [Tramèr *et al.*, 2017] Florian Tramèr, Alexey Kurakin, Nicolas Papernot, Ian Goodfellow, Dan Boneh, and Patrick McDaniel. Ensemble adversarial training: Attacks and defenses. *arXiv preprint arXiv:1705.07204*, 2017.
- [Wang and He, 2021] Xiaosen Wang and Kun He. Enhancing the transferability of adversarial attacks through variance tuning. In *Proceedings of the IEEE/CVF conference on computer vision and pattern recognition*, pages 1924–1933, 2021.
- [Wang *et al.*, 2019] Jingyi Wang, Guoliang Dong, Jun Sun, Xinyu Wang, and Peixin Zhang. Adversarial sample detection for deep neural network through model mutation testing. In *2019 IEEE/ACM 41st International Conference on Software Engineering (ICSE)*, pages 1245–1256. IEEE, 2019.
- [Wang *et al.*, 2021a] Xiaosen Wang, Xuanran He, Jingdong Wang, and Kun He. Admix: Enhancing the transferability of adversarial attacks. In *Proceedings of the IEEE/CVF International Conference on Computer Vision*, pages 16158–16167, 2021.
- [Wang *et al.*, 2021b] Xiaosen Wang, Jiadong Lin, Han Hu, Jingdong Wang, and Kun He. Boosting adversarial transferability through enhanced momentum. *arXiv preprint arXiv:2103.10609*, 2021.
- [Wang *et al.*, 2023] Donghua Wang, Wen Yao, Tingsong Jiang, and Xiaoqian Chen. Improving transferability of universal adversarial perturbation with feature disruption. *IEEE Transactions on Image Processing*, 2023.
- [Wightman, 2019] Ross Wightman. Pytorch image models. <https://github.com/rwightman/pytorch-image-models>, 2019.
- [Xiao *et al.*, 2021] Zihao Xiao, Xianfeng Gao, Chilin Fu, Yinpeng Dong, Wei Gao, Xiaolu Zhang, Jun Zhou, and Jun Zhu. Improving transferability of adversarial patches on face recognition with generative models. In *Proceedings of the IEEE/CVF conference on computer vision and pattern recognition*, pages 11845–11854, 2021.
- [Xie *et al.*, 2017] Saining Xie, Ross Girshick, Piotr Dollár, Zhuowen Tu, and Kaiming He. Aggregated residual transformations for deep neural networks. In *Proceedings of the IEEE conference on computer vision and pattern recognition*, pages 1492–1500, 2017.
- [Xie *et al.*, 2019] Cihang Xie, Zhishuai Zhang, Yuyin Zhou, Song Bai, Jianyu Wang, Zhou Ren, and Alan L Yuille. Improving transferability of adversarial examples with input diversity. In *Proceedings of the IEEE/CVF conference on computer vision and pattern recognition*, pages 2730–2739, 2019.
- [Xiong *et al.*, 2022] Yifeng Xiong, Jiadong Lin, Min Zhang, John E Hopcroft, and Kun He. Stochastic variance reduced ensemble adversarial attack for boosting the adversarial transferability. In *Proceedings of the IEEE/CVF conference on computer vision and pattern recognition*, pages 14983–14992, 2022.
- [Yuan *et al.*, 2024] Zheng Yuan, Jie Zhang, Zhaoyan Jiang, Liangliang Li, and Shiguang Shan. Adaptive perturbation for adversarial attack. *IEEE Transactions on Pattern Analysis and Machine Intelligence*, 2024.
- [Zhang *et al.*, 2022] Jianping Zhang, Weibin Wu, Jen-tse Huang, Yizhan Huang, Wenxuan Wang, Yuxin Su, and Michael R Lyu. Improving adversarial transferability via neuron attribution-based attacks. In *Proceedings of the IEEE/CVF Conference on Computer Vision and Pattern Recognition*, pages 14993–15002, 2022.
- [Zhao *et al.*, 2018] Zhengli Zhao, Dheeru Dua, and Sameer Singh. Generating natural adversarial examples. In *International Conference on Learning Representations*, 2018.
- [Zheng and Hong, 2018] Zhihao Zheng and Pengyu Hong. Robust detection of adversarial attacks by modeling the intrinsic properties of deep neural networks. *Advances in neural information processing systems*, 31, 2018.

Supplementary Material

A Algorithm

Taking MIFGSM as an example, the specific algorithmic workflow of MIFGSM-IKD is detailed in Algorithm 1. By incorporating the momentum term and an appropriate IKD strategy, adversarial samples are iteratively updated to achieve effective attacks on the target model.

Algorithm 1 Example algorithm

Input: A classifier f with loss function \mathcal{L} ; a benign sample x and ground-truth label y ;

Input: The size of perturbation ϵ ; iterations T and decay factor μ

Output: An adversarial sample x^{adv} with $\|x^{adv} - x\|_\infty \leq \epsilon$.

- 1: $\alpha = \frac{\epsilon}{T}$;
- 2: $g_0 = 0; x_0^{adv} = x$;
- 3: **for** $t = 0$ to $T - 1$ **do**
- 4: Input x_t^{adv} to f and obtain the hard label loss $\mathcal{L}_{hard}(f_\varphi(x_t^{adv}), y)$;
- 5: Input x_t^{adv} and x to f and obtain the soft label loss $\mathcal{L}_{soft}(f_\varphi(x_t^{adv}), f_\varphi(x))$;
- 6: Calculate the total loss
$$\mathcal{L}_{total} = \mathcal{L}_{hard}(f_\varphi(x_t^{adv}), y) + \gamma \mathcal{L}_{soft}(f_\varphi(x_t^{adv}), f_\varphi(x));$$
- 7: Obtain the gradient $\nabla_x(\mathcal{L}_{total})$;
- 8: Update g_{t+1} by accumulating the velocity vector in the gradient direction as

$$g_{t+1} = \mu \cdot g_t + \frac{\nabla_x(\mathcal{L}_{total})}{\|\nabla_x(\mathcal{L}_{total})\|_1};$$

- 9: Update x_{t+1}^{adv} by applying the sign gradient as

$$x_{t+1}^{adv} = x_t^{adv} + \alpha \cdot \text{sign}(g_{t+1});$$

10: **end for**

11: **return** $x^{adv} = x_t^{adv}$.

B Experiments

Table 3 demonstrates the effects of IKD on classical and input transformation-based attacks when using ResNeXt50, Inception-v3, Inception-v4, and ResNet152 as surrogate models.

Table 4 illustrates the impact of IKD on advanced gradient attacks using ResNeXt50, Inception-v3, Inception-v4, and ResNet152 as surrogate models.

Table 5 presents the impact of different IKD methods on the success rate of transfer-based attacks, with ResNet50 serving as the surrogate model.

Tables 6 and 7 presents the effect of IKD weight on the transfer-based attack success rate.

Table 3: Comparison results of various attack methods in terms of attack success rate (%). The bold item indicates the best one. Item with * superscript is white-box attacks, and the others is black-box attacks. AVG column indicates the average attack success rate on black-box models.

Source Model	Method	Target Model											AVG
		RN50	DN121	RNX50	VGG19BN	IncRes-v2	Inc-v3	Inc-v4	RN101	RN152	Inc-v3 _{adv}	IncRes-V2 _{adv,ens}	
RNX50	MIFGSM	68.2	60.6	98.7*	72.8	31.3	46.1	40.1	61.8	55.2	35.7	15.5	48.7
	MIFGSM-IKD	72.0	63.3	98.9*	72.2	34.0	45.1	41.6	64.8	57.9	35.9	14.9	50.2
	DIFGSM	79.0	75.9	94.6*	78.5	52.2	59.7	62.1	75.8	71.9	36.3	16.1	60.8
	DIFGSM-IKD	81.3	76.3	96.1*	81.9	55.1	60.2	62.0	77.2	73.1	37.4	17.5	62.2
	TIFGSM	54.6	58.0	85.6*	67.5	42.2	54.6	52.1	45.8	41.2	42.0	33.1	49.1
	TIFGSM-IKD	54.6	56.6	85.5*	68.0	42.6	55.0	52.2	45.2	41.1	41.8	35.6	49.3
	NIFGSM	74.8	67.8	99.9*	73.9	35.5	47.0	46.3	67.4	61.0	37.6	14.8	52.6
	NIFGSM-IKD	78.5	70.2	99.8*	77.7	37.1	49.3	44.2	69.6	63.8	36.0	13.6	54.0
Inc-v3	MIFGSM	47.7	60.9	44.7	72.3	58.3	99.1*	61.8	38.3	35.9	41.5	21.4	48.3
	MIFGSM-IKD	48.6	60.0	45.1	72.4	58.1	99.7*	62.8	38.6	36.6	41.8	22.6	48.7
	DIFGSM	56.6	68.6	53.3	78.7	70.1	99.1*	73.8	47.2	42.0	49.5	26.9	56.7
	DIFGSM-IKD	57.8	69.5	56.1	79.8	74.9	99.3*	77.2	50.9	45.2	54.0	29.0	59.4
	TIFGSM	32.7	49.8	28.6	64.2	51.2	98.8*	60.0	21.0	18.8	56.0	42.4	42.5
	TIFGSM-IKD	33.9	50.4	30.9	66.6	55.9	98.7*	62.4	23.0	20.3	60.3	44.9	44.9
	NIFGSM	55.4	69.4	52.0	76.5	64.9	99.4*	70.0	47.7	40.8	42.2	21.6	54.1
	NIFGSM-IKD	57.6	71.5	56.3	78.4	69.5	99.8*	72.7	48.1	45.6	44.3	23.0	56.7
Inc-v4	MIFGSM	53.3	62.4	52.8	76.5	60.4	69.5	97.9*	45.0	42.6	37.1	20.4	52.0
	MIFGSM-IKD	54.1	64.2	53.7	78.9	62.2	71.8	99.0*	48.3	44.7	38.4	20.1	53.6
	DIFGSM	62.9	70.9	62.1	82.4	76.2	79.8	98.0*	55.6	52.4	45.2	25.6	61.3
	DIFGSM-IKD	66.2	74.0	66.7	84.4	76.2	81.6	98.1*	59.4	55.7	47.7	26.7	63.9
	TIFGSM	39.3	51.4	37.2	67.7	55.9	67.5	97.7*	27.8	24.1	53.1	44.5	46.9
	TIFGSM-IKD	40.0	52.2	38.0	69.1	57.8	70.1	97.1*	28.9	25.7	55.7	44.2	48.2
	NIFGSM	58.5	66.4	58.3	82.5	61.6	72.3	98.9*	49.6	45.3	37.4	18.9	55.1
	NIFGSM-IKD	60.8	69.1	60.2	82.6	65.7	74.8	99.8*	52.7	48.9	39.3	20.7	57.5
RN152	MIFGSM	69.6	62.9	66.3	74.1	35.9	48.7	42.2	68.8	96.2*	26.2	14.8	51.0
	MIFGSM-IKD	71.2	63.5	68.8	74.8	38.1	49.7	44.7	70.3	96.4*	27.4	14.9	52.3
	DIFGSM	75.2	72.3	75.5	79.0	55.4	62.7	60.5	78.0	91.2*	33.7	17.6	61.0
	DIFGSM-IKD	76.3	72.0	77.6	78.0	55.2	62.5	60.8	78.7	91.8*	32.9	17.8	61.2
	TIFGSM	49.4	52.4	50.5	64.1	42.1	54.5	49.0	49.4	74.4*	42.6	36.8	49.1
	TIFGSM-IKD	50.8	51.4	51.6	62.8	42.2	53.2	50.0	51.0	74.9*	42.4	35.1	49.1
	NIFGSM	77.3	68.0	74.5	77.4	37.0	51.1	44.3	76.4	99.1*	27.4	15.6	54.9
	NIFGSM-IKD	78.8	70.7	75.0	79.5	38.4	51.0	45.6	77.5	99.1*	26.6	15.1	55.8

Table 4: Evaluation results of the advanced attacks combined with IKD in terms of attack success rate (%). The bold item indicates the best one. Item with * superscript is white-box attacks, and the others is black-box attacks. AVG column indicates the average attack success rate on black-box models.

Source Model	Method	Target Model											AVG
		RN50	DN121	RNX50	VGG19BN	IncRes-v2	Inc-v3	Inc-v4	RN101	RN152	Inc-v3 _{adv}	IncRes-V2 _{adv,ens}	
RNX50	SINIFGSM	91.0	88.5	99.9*	86.8	61.2	70.0	70.1	87.5	82.9	39.3	18.5	69.6
	SINIFGSM-IKD	91.7	87.6	99.9*	87.0	61.9	69.8	68.9	87.9	85.0	38.2	18.3	69.6
	VMIFGSM	81.5	77.8	97.1*	81.1	59.2	66.3	66.9	77.9	75.3	40.0	23.9	65.0
	VMIFGSM-IKD	81.4	78.1	98.1*	80.7	59.2	67.2	67.5	78.8	76.6	39.8	23.0	65.2
	VNIFGSM	82.4	79.8	97.1*	82.5	61.9	68.8	68.1	78.8	77.2	41.9	23.5	66.5
Inc-v3	VNIFGSM-IKD	82.0	79.5	98.0*	80.9	60.6	70.3	66.9	78.4	77.1	40.3	22.3	65.8
	SINIFGSM	56.3	71.2	53.5	83.4	67.6	100.0*	72.5	45.7	42.6	50.2	26.2	56.9
	SINIFGSM-IKD	62.4	74.4	57.7	84.4	74.7	100.0*	78.1	50.9	47.1	54.7	25.3	61.0
	VMIFGSM	55.8	68.8	53.9	78.2	73.0	99.4*	73.4	48.7	43.4	52.9	29.5	57.8
	VMIFGSM-IKD	58.9	70.7	54.4	79.2	75.0	99.4*	78.4	51.3	47.5	56.7	30.4	60.3
Inc-v4	VNIFGSM	61.3	72.2	57.5	80.2	75.2	99.7*	77.7	50.4	47.4	53.6	31.3	60.7
	VNIFGSM-IKD	64.7	76.4	61.9	82.9	79.9	100.0*	83.2	56.4	52.5	59.0	33.1	65.0
	SINIFGSM	67.3	79.6	66.0	90.0	80.2	87.9	100.0*	61.3	57.5	59.3	34.9	68.4
	SINIFGSM-IKD	73.6	83.0	71.3	92.3	85.7	90.2	99.9*	66.2	62.7	61.0	35.0	72.1
	VMIFGSM	60.9	69.7	60.0	81.3	73.6	78.9	98.6*	55.9	54.5	50.5	29.7	61.5
RN152	VMIFGSM-IKD	65.7	73.1	65.6	83.4	79.6	82.9	98.5*	60.2	60.3	52.0	31.3	65.4
	VNIFGSM	65.3	73.5	63.8	85.0	77.6	82.2	99.5*	56.4	55.6	52.1	29.8	64.1
	VNIFGSM-IKD	70.3	77.0	70.7	87.3	82.1	85.3	99.8*	64.6	62.3	53.5	31.9	68.5
	SINIFGSM	91.1	87.0	88.4	87.4	65.1	71.8	70.7	91.4	99.5*	40.4	20.1	71.3
	SINIFGSM-IKD	91.5	88.1	89.2	86.4	63.6	71.9	69.6	90.7	99.2*	39.0	19.3	70.9
RN152	VMIFGSM	78.5	72.0	76.8	79.0	58.1	63.5	62.9	77.0	95.8*	40.0	23.4	63.1
	VMIFGSM-IKD	78.6	72.2	77.7	78.8	57.6	64.7	62.0	78.0	95.7*	39.7	23.7	63.3
	VNIFGSM	81.6	76.4	81.2	82.0	61.1	65.7	66.2	80.3	97.4*	40.0	24.0	65.9
	VNIFGSM-IKD	82.1	78.0	81.3	82.1	61.0	67.5	65.9	81.5	98.0*	39.9	24.8	66.4

Table 5: Comparison results of various attack methods under different IKD methods regarding attack success rate (%). The bold item indicates the best, and the underlined item indicates the suboptimal. An item with * superscript is a white-box attack; the others are black-box attacks. The AVG column indicates the average attack success rate on black-box models. The source model is ResNet50 and the IKD weight is 0.01.

Method	Target Model										
	RN50	DN121	RNX50	VGG19BN	IncRes-v2	Inc-v3	Inc-v4	RN101	RN152	Inc-v3 _{adv}	IncRes-V2 _{adv, ens}
MIFGSM	99.9*	65.7	<u>75.2</u>	73.2	38.9	52.6	46.0	68.2	62.1	30.6	16.0
MIFGSM-IKD(CE)	99.9*	<u>66.6</u>	74.2	73.0	38.8	<u>53.6</u>	46.0	69.4	<u>63.6</u>	30.7	<u>16.2</u>
MIFGSM-IKD(MSE)	99.9*	65.4	74.1	<u>73.6</u>	37.2	53.2	<u>46.2</u>	68.0	62.4	<u>31.3</u>	15.9
MIFGSM-IKD(KL)	99.9*	68.4	79.4	76.0	39.9	54.4	49.6	73.1	67.6	32.1	16.3
DIFGSM	99.9*	82.9	88.8	<u>84.7</u>	61.7	70.3	69.4	<u>86.1</u>	<u>82.1</u>	35.9	18.4
DIFGSM-IKD(CE)	99.8*	83.9	<u>88.9</u>	83.4	61.0	<u>70.5</u>	68.4	83.5	80.2	38.1	18.4
DIFGSM-IKD(MSE)	<u>99.8*</u>	83.8	88.4	83.4	60.4	70.1	69.0	83.9	80.7	36.2	19.0
DIFGSM-IKD(KL)	99.8*	84.9	90.6	84.8	62.9	70.8	69.6	86.5	83.3	38.4	18.9
TIFGSM	99.0*	<u>68.4</u>	<u>65.4</u>	<u>71.3</u>	51.1	63.9	<u>60.3</u>	55.6	49.8	52.8	<u>43.0</u>
TIFGSM-IKD(CE)	98.9*	67.2	64.6	71.8	51.6	64.2	59.6	54.5	47.0	50.7	41.7
TIFGSM-IKD(MSE)	<u>99.1*</u>	67.2	64.9	70.9	50.9	63.3	59.1	<u>55.8</u>	47.8	<u>51.3</u>	42.2
TIFGSM-IKD(KL)	99.2*	69.1	67.1	70.8	52.1	64.5	61.4	57.9	49.5	52.8	43.8
NIFGSM	99.9*	71.6	80.0	76.5	43.4	55.2	<u>49.2</u>	75.9	70.7	<u>31.6</u>	<u>16.0</u>
NIFGSM-IKD(CE)	100.0*	71.2	80.7	<u>77.4</u>	42.3	<u>57.2</u>	49.1	76.6	71.6	32.0	16.4
NIFGSM-IKD(MSE)	99.9*	<u>72.7</u>	81.0	<u>77.2</u>	44.2	55.6	48.9	76.8	<u>71.7</u>	31.1	16.4
NIFGSM-IKD(KL)	100.0*	76.5	85.0	79.3	44.6	57.8	52.5	81.1	74.7	32.0	15.4
SINIFGSM	99.9*	81.7	85.0	84.5	53.2	67.0	59.3	<u>80.1</u>	75.4	37.6	17.1
SINIFGSM-IKD(CE)	99.9*	<u>83.4</u>	<u>85.3</u>	84.7	<u>54.3</u>	67.1	<u>60.8</u>	<u>80.1</u>	74.9	36.5	17.8
SINIFGSM-IKD(MSE)	99.8*	82.6	84.4	85.4	53.4	67.2	60.5	79.2	76.6	37.9	17.5
SINIFGSM-IKD(KL)	100.0*	88.5	91.3	88.7	58.0	69.9	64.5	87.9	84.1	38.2	<u>17.7</u>
VMIFGSM	99.9*	84.9	88.6	86.5	64.8	<u>73.6</u>	73.5	<u>85.5</u>	84.9	43.8	24.2
VMIFGSM-IKD(CE)	99.9*	85.9	88.2	<u>86.4</u>	66.4	73.7	72.9	<u>85.5</u>	85.5	<u>44.5</u>	<u>23.8</u>
VMIFGSM-IKD(MSE)	99.8*	<u>85.9</u>	88.2	86.1	65.2	73.1	<u>73.0</u>	85.3	85.2	44.0	23.2
VMIFGSM-IKD(KL)	99.9*	86.1	89.3	86.1	<u>65.6</u>	72.6	72.6	87.1	<u>85.3</u>	44.7	23.4
VNIFGSM	99.9*	<u>86.2</u>	89.2	87.0	68.7	74.1	<u>73.1</u>	87.2	86.0	45.0	23.0
VNIFGSM-IKD(CE)	99.9*	<u>86.2</u>	89.9	<u>87.5</u>	67.5	75.4	73.0	87.6	<u>86.5</u>	44.2	23.4
VNIFGSM-IKD(MSE)	99.9*	86.0	<u>90.5</u>	86.7	<u>68.0</u>	74.6	72.6	87.5	85.9	44.1	23.3
VNIFGSM-IKD(KL)	<u>99.8*</u>	86.6	91.1	88.2	68.7	<u>75.3</u>	74.0	88.8	88.0	<u>44.3</u>	24.2

Table 6: Comparison results of various attack methods under different IKD weights regarding attack success rate (%). The bold item indicates the best, and the underlined item indicates the suboptimal. An item with * superscript is white-box attack; the others are black-box attacks. The source model is ResNet50 and the distillation method is KL divergence.

Method	Weight	Target Model											
		RN50	DN121	RNX50	VGG19BN	IncRes-v2	Inc-v3	Inc-v4	RN101	RN152	Inc-v3 _{adv}	IncRes-V2 _{adv, ens}	
MIFGSM	/	99.9*	65.7	75.2	73.2	38.9	52.6	46.0	68.2	62.1	30.6	16.0	
	1000	81.2*	58.9	65.6	65.9	33.9	47.3	41.8	62.0	58.4	30.7	15.3	
	100	94.2*	66.1	74.1	71.7	39.4	51.1	48.1	69.4	65.8	32.1	15.5	
	10	99.9*	69.5	78.5	<u>75.7</u>	40.2	54.6	49.2	73.3	68.5	31.3	<u>16.7</u>	
	1	99.9*	<u>69.1</u>	79.3	75.1	<u>40.7</u>	53.9	48.6	74.3	66.9	32.1	16.5	
	0.01	99.9*	68.5	79.3	76.0	41.0	53.8	49.8	72.4	67.4	31.1	15.7	
MIFGSM-IKD	0.001	99.9*	68.4	<u>79.4</u>	76.0	39.9	<u>54.4</u>	<u>49.6</u>	73.1	<u>67.6</u>	32.1	16.3	
	0.001	99.9*	69.5	79.8	74.6	40.5	52.6	49.2	<u>73.3</u>	67.4	31.5	17.1	
	DIFGSM	/	99.9*	82.9	88.8	<u>84.7</u>	61.7	70.3	69.4	<u>86.1</u>	82.1	35.9	18.4
		1000	67.2*	58.2	61.0	64.1	43.2	51.2	47.7	58.2	57.2	30.2	14.7
		100	74.4*	63.8	67.6	68.2	47.0	54.3	52.5	64.9	62.8	31.9	16.2
		10	78.8*	68.0	70.0	71.5	50.2	56.9	56.2	67.8	66.3	31.6	17.2
1		89.1*	76.7	81.0	77.8	56.0	63.8	61.8	77.2	75.0	34.7	16.8	
0.1		98.1*	83.9	88.7	82.8	62.2	<u>71.6</u>	69.4	85.8	82.7	37.5	<u>18.7</u>	
DIFGSM-IKD	0.01	99.8*	84.9	90.6	84.8	62.9	70.8	69.6	86.5	83.3	38.4	18.9	
	0.001	99.7*	85.0	<u>89.8</u>	84.3	63.7	72.5	70.5	86.5	83.7	<u>37.6</u>	18.5	
	TIFGSM	/	99.0*	68.4	65.4	71.3	51.1	63.9	60.3	55.6	49.8	52.8	43.0
		1000	66.6*	47.0	46.6	55.1	37.0	47.9	44.1	38.8	35.1	38.4	31.2
		100	73.4*	52.1	50.8	59.1	40.5	49.8	46.4	41.5	37.8	41.3	33.1
		10	78.0*	54.4	53.3	62.2	41.6	52.3	49.7	44.1	39.1	43.6	33.8
1		88.3*	61.6	60.1	66.0	46.4	58.9	55.0	50.3	43.5	46.9	38.5	
0.1		98.1*	68.2	66.8	<u>71.4</u>	52.8	64.0	60.2	55.4	48.4	52.3	42.7	
TIFGSM-IKD	0.01	99.2*	69.1	67.1	70.8	52.1	64.5	<u>61.4</u>	57.9	<u>49.5</u>	52.8	43.8	
	0.001	99.1*	<u>68.6</u>	<u>66.8</u>	71.6	53.3	64.0	61.7	<u>57.5</u>	48.4	<u>52.6</u>	42.2	
	NIFGSM	/	99.9*	71.6	80.0	76.5	43.4	55.2	49.2	75.9	70.7	31.6	16.0
		1000	87.8*	66.6	74.1	71.9	40.0	51.7	47.5	71.2	65.3	30.4	15.1
		100	96.2*	72.6	80.6	75.0	43.5	55.7	51.8	77.9	72.7	31.6	15.6
		10	99.9*	75.8	83.8	79.8	45.0	59.0	53.1	81.8	76.0	31.9	14.9
1		99.9*	75.3	<u>84.8</u>	78.5	<u>45.0</u>	58.1	53.0	80.7	74.2	32.4	15.5	
0.1		<u>99.9*</u>	<u>76.4</u>	84.6	79.0	44.1	57.9	<u>53.7</u>	80.8	76.0	31.6	15.4	
NIFGSM-IKD	0.01	100.0*	76.5	85.0	<u>79.3</u>	44.6	57.8	52.5	<u>81.1</u>	74.7	<u>32.0</u>	15.4	
	0.001	100.0*	75.2	85.0	79.0	45.9	<u>58.8</u>	54.2	79.1	<u>75.7</u>	31.8	16.0	

Table 7: Evaluation results of the advanced attacks under different IKD weights regarding attack success rate (%). The bold item indicates the best, and the underlined item indicates the suboptimal. An item with \star superscript is white-box attack, the others are black-box attacks. The source model is ResNet50 and the IKD method is KL divergence.

Method	Weight	Target Model										
		RN50	DN121	RNX50	VGG19BN	IncRes-v2	Inc-v3	Inc-v4	RN101	RN152	Inc-v3 adv	IncRes-V2 adv, ens
SINIFGSM	/	<u>99.9\star</u>	81.7	85.0	84.5	53.2	67.0	59.3	80.1	75.4	<u>37.6</u>	17.1
	1000	97.2 \star	84.1	84.5	87.5	52.8	66.9	62.3	82.3	78.3	35.6	17.6
	100	97.2 \star	82.8	85.3	87.0	51.6	65.4	62.2	81.7	77.2	34.7	17.0
	10	97.7 \star	84.2	85.6	87.2	53.8	66.5	63.5	81.6	77.3	35.2	16.6
SINIFGSM-IKD	1	<u>99.9\star</u>	85.5	88.8	88.4	55.1	69.0	65.8	84.8	81.1	36.1	17.0
	0.1	99.8 \star	85.9	90.0	87.7	57.6	70.3	64.2	<u>87.0</u>	82.7	36.3	18.4
	0.01	100.0\star	88.5	<u>91.3</u>	88.7	58.0	69.9	64.5	87.9	<u>84.1</u>	38.2	17.7
	0.001	99.9 \star	<u>87.2</u>	91.7	<u>88.5</u>	<u>57.9</u>	70.3	<u>65.5</u>	87.9	84.5	37.5	<u>18.0</u>
VMIFGSM	/	99.9\star	84.9	88.6	86.5	64.8	73.6	<u>73.5</u>	85.5	84.9	43.8	24.2
	1000	91.0 \star	78.0	82.7	79.2	57.9	65.4	64.7	80.0	78.0	38.3	19.4
	100	98.2 \star	82.6	87.5	83.8	59.7	67.9	66.5	84.7	82.9	39.3	20.1
	10	<u>99.7\star</u>	83.4	88.7	83.5	60.3	68.0	68.3	86.7	84.6	38.7	20.4
VMIFGSM-IKD	1	<u>99.7\star</u>	83.9	<u>90.5</u>	84.5	61.8	69.0	68.6	86.5	84.5	40.2	20.4
	0.1	99.9\star	85.0	90.6	85.4	64.3	71.0	70.8	86.9	84.9	42.5	21.9
	0.01	99.9\star	<u>86.1</u>	89.3	86.1	<u>65.6</u>	72.6	72.6	<u>87.1</u>	<u>85.3</u>	44.7	<u>23.4</u>
	0.001	99.9\star	86.9	89.1	<u>86.2</u>	66.9	<u>73.3</u>	73.6	87.3	85.9	<u>44.4</u>	23.3
VNIFGSM	/	99.9\star	86.2	89.2	87.0	68.7	74.1	73.1	87.2	86.0	<u>45.0</u>	23.0
	1000	93.8 \star	83.5	87.2	83.4	62.1	70.9	70.4	85.5	82.8	40.1	18.3
	100	98.3 \star	86.3	92.1	85.6	64.3	72.3	72.2	89.1	86.2	39.8	19.4
	10	99.7 \star	87.0	92.6	86.6	65.5	74.0	72.0	89.6	87.8	40.5	19.1
VNIFGSM-IKD	1	99.8 \star	87.6	<u>92.5</u>	87.4	66.2	73.8	73.6	90.4	<u>88.3</u>	40.2	20.6
	0.1	99.9\star	<u>87.4</u>	92.2	<u>87.7</u>	68.3	76.3	73.9	<u>90.1</u>	88.9	42.2	21.8
	0.01	99.8 \star	86.6	91.1	88.2	68.7	<u>75.3</u>	<u>74.0</u>	88.8	88.0	44.3	24.2
	0.001	99.7 \star	87.2	90.9	<u>87.7</u>	<u>68.5</u>	75.0	74.5	88.1	87.4	45.4	<u>23.5</u>